Am J Cancer Res 2020;10(6):1710-1727
www.ajcr.us /ISSN:2156-6976/ajcr0109962

Original Article

NADPH oxidase 5α promotes the formation of CD271 tumor-initiating cells in oral cancer

Wei Gao[1*], Shaowei Xu[2*], Minjuan Zhang[1], Shuai Liu[1], Sharie Pui-Kei Siu[1], Hanwei Peng[2], Judy Chun-Wai Ng[1], George Sai-Wah Tsao[3], Anthony Wing-Hung Chan[4], Velda Ling-Yu Chow[1], Jimmy Yu-Wai Chan[1], Thian-Sze Wong[1]

[1]Department of Surgery, LKS Faculty of Medicine, The University of Hong Kong, 21 Sassoon Road, Pokfulam, Hong Kong, China; [2]Department of Head and Neck Surgery, Cancer Hospital of Shantou University Medical College, 7 Raoping Road, Shantou 515031, Guangdong Province, China; [3]School of Biomedical Sciences, LKS Faculty of Medicine, The University of Hong Kong, 21 Sassoon Road, Pokfulam, Hong Kong, China; [4]Department of Anatomical and Cellular Pathology, The Chinese University of Hong Kong, 30-32 Ngan Shing Street, Shatin, NT, China. [*]Equal contributors.

Received February 27, 2020; Accepted March 31, 2020; Epub June 1, 2020; Published June 15, 2020

Abstract: Oral tongue squamous cell carcinoma (OTSCC) has a distinctive cell sub-population known as tumor-initiating cells (TICs). CD271 is a functional TIC receptor in head and neck cancers. The molecular mechanisms governing CD271 up-regulation remains unclear. Oxidative stress is a contributing factor in TIC development. Here, we explored the potential role of NADPH oxidase 5 (NOX5) and its regulatory mechanism on the development of CD271-expressing OTSCC. Our results showed that the splice variant NOX5α is the most prevalent form expressed in head and neck cancers. NOX5α enhanced OTSCC proliferation, migration, and invasion. Overexpression of NOX5α increased the size of OTSCC xenograft significantly in vivo. The tumor-promoting functions of NOX5α were mediated through the reactive oxygen species (ROS)-generating property. NOX5α activated ERK singling and increased CD271 expression at the transcription level. Also, NOX5α reduces the sensitivity of OTSCC to cisplatin and natural killer cells. The findings indicate that NOX5α plays an important part in the development of TIC in OTSCC.

Keywords: NADPH oxidase 5, tumor-initiating cells, cisplatin, natural killer cells, reactive oxygen species

Introduction

Oral squamous cell carcinoma (OTSCC) in the oral mucosal epithelium is a poor prognostic disease with a 5-year survival rate of around 50%. The tumor mass consists of a heterogeneous population of epithelial cancer cells with different tumor-forming ability. In 2004, Mackenzie observed a subpopulation of OTSCC with a distinctive growth pattern in 3D organotypic cultures [1]. They have a remarkable high expansion propensity to form tumor mass. It is now recognized that OTSCC contains a distinctive cell sub-population known as tumor-initiating cells (TICs). TIC has a high tumor formation ability in xenotransplantation studies at low cell numbers. TIC with high expression of stem cell markers can persist after chemotherapy or radiotherapy. Hence, selective targeting of TIC is critical for the treatment outcome and long-term prognosis.

CD271 or p75(NTR) is a heterodimeric surface receptor that belongs to the tumor necrosis factor receptor superfamily. CD271 is a TIC marker of melanoma responsible for chemotherapy resistance. In oral mucosal, CD271 is detected in the basement membrane [2]. CD271 expression is also found in the stem- or progenitor-cell lineages of human oral keratinocytes. CD271 positive cells have higher proliferation and clonal growth ability. High CD271 expression is found in oral cancer with less differentiated phenotype [3]. Imai et al. reported that CD271 positive population in carcinoma derived from the hypopharyngeal region has high tumor-forming capacity in the immunocompromised mice [4]. Current data suggest that CD271 is a functional TIC marker of epithelial cancer in the head and neck regions.

Alterations of free radicals/reactive oxygen species (ROS) and antioxidants have clear function-

al implications on precancer carcinogenesis and oral cancers [5]. ROS can be free radicals as well as non-radical derivatives of oxygen. Due to the reactive nature of ROS, ROS could damage genetic materials contributing to the cumulative mutations which promote cancer initiation and progression. High ROS promotes cancer metastasis and angiogenesis [6]. ROS can promote tumor progression and survival by functioning as a signaling molecule that activates key oncogenic singling pathways. In oral cancer patients, a reduced level of anti-oxidative enzymes such as SOD and catalase was observed [7]. Further, ROS generated from tobacco is considered to be exogenous ROS sources which contribute to the oxidative stress associated with OTSCC tumorigenesis. The inhibitory effect of antioxidants on oral cancers suggesting that ROS is a putative target for OTSCC treatment [8, 9].

ROS can be derived from exogenous and endogenous sources. In mammalian cells, NADPH oxidase (NOX) family members are major endogenous ROS sources. NOX members (NOX1, NOX2, NOX3, NOX4, NOX5, and DUOX1/2) are highly conserved transmembrane catalytic subunits which expression is tissue/organ-specific. Also, NOX members have a different regulatory mechanism on their enzymatic activity. Most NOX members need to interact with different cytosolic activator to maintain their enzymatic activity. NOX5, however, can produce and release ROS independently [10]. NOX5 protein is catalytically active with no membrane or cytosolic subunit [11, 12]. Thus, the ROS-generating activity of NOX5 can be controlled directly by the protein expression level. NOX5 can generate radical and non-radical ROS. NOX5 is an essential mediator in vascular and cardiovascular disease [13]. Due to the high expression in solid cancer, it is speculated that NOX5 is involved in regulating tumor growth and survival [14, 15]. In mammalian cells, NOX5 has six isoforms [Nox5-α, -β, -δ, -γ, -ζ, and -ε] (short) with restricted tissue expression patterns. At present, the pathological impact of the NOX5 isoforms in oral cancer remains poorly understood.

At present, the molecular mechanism controlling CD271 expression in OTSCC remains unclear. There is a clear link between ROS and TIC-associated pathological features in head and neck cancer [16]. Residual TIC remained after chemotherapy/radiotherapy is directly linked to the high recurrence and poor prognosis of OTSCC. Thus, we here explored the potential role of NOX5 and its regulatory effects on the development of TIC in OTSCC.

Materials and methods

Cell culture and reagents

CAL27 and YD-38 (OTSCC cell lines) were used. CAL27, a tongue squamous cell carcinoma cell line originated from the middle of the tongue, was obtained from the American Type Culture Collection (ATCC). YD38, an oral squamous cell carcinoma cell line originated from the lower gingiva, was obtained from the Korean cell line bank. KHYG-1, a human natural killer cell line derived from NK cell leukemia, was obtained from Japanese Collection of Research Bioresources Cell Bank. OTSCC cells were cultured in RPMI Medium 1640 (Gibco, NY, USA) supplemented with 10% fetal bovine serum (FBS, Gibco) and 1% antibiotic-antimycotic (Gibco). KHYG-1 cells were cultured in RPMI Medium 1640 (Gibco) supplemented with 10% fetal bovine serum (Gibco), 1% antibiotic-antimycotic (Gibco) and 100 units/ml of rIL-2 (R&D Systems, MN, Canada). Cells were incubated in humidified incubator at 37°C under 5% CO_2. Tempol (4-hydroxy-2,2,6,6-tetramethylpiperidin-1-oxyl, Sigma Aldrich, MO, USA) was used to treat CAL27 and YD38 cells at a concentration of 0.5 mM for 48 hours. Cisplatin [cis-Diammineplatinum (II) dichloride, Sigma Aldrich, MO, USA] was used to treat OTSCC cells at the concentration of 2-8 μM for 72 hours.

Generation of NOX5α-overexpressing OTSCC cell lines

NOX5α-overexpressing vector containing full-length human NOX5α fragment (2214-bp, NM_001184779.2) and mock lentivector were custom made from VectorBuilder Inc. (IL, USA). pPACKH1 HIV Lentivector Packaging Kit (System Biosciences, CA, USA) was used for lentivirus packaging. TransDux™ MAX Lentivirus Transduction Reagent (System Biosciences) was used for the lentivirus transduction of CAL27 and YD-38 cells.

Quantitative polymerase chain reaction (QPCR)

TRIzol reagent (Thermo Fisher Scientific, MA, USA) was used to extract RNA. Reverse tran-

scription was carried out using PrimeScript RT reagent Kit with gDNA Eraser (Takara, CA, USA). Primers and probes were designed by using the Universal ProbeLibrary Assay Design Center (http://www.roche-applied-science.com/). Primers sequence and probes were as follows: NOX5-forward, 5'-CGAGGAGGCTCAATACGG-3'; NOX5-reverse, 5'-TCTTGCCCAGTGCAGATGT-3'; NOX5-probe, #1; CD271-forward, 5'-GGGATGGTACTAGGGGGAAG-3'; CD271-reverse, 5'-GCTCTGGTTCCTCGATTCCT-3'; CD271-probe, #57; OCT4-forward, 5'-TTGGGCTCGAGAAGGATGT-3'; OCT4-reverse, 5'-GGTCCCCCTGAGAAAGGA-3'; OCT4-probe, #3; GAPDH-forward, 5'-AGCCACATCGCTCAGACAC-3'; GAPDH-reverse, 5'-GCCCAATACGACCAAATCC-3'; GAPDH-probe, #60.

QPCR was performed using FastStart Universal Probe Master (Roche Applied Science, Penzberg, Germany) on a LightCycler® 480 (Roche Applied Science). PCR conditions were as follows: 95°C for 10 minutes, followed by 45 cycles of 95°C for 15 seconds and 60°C for 1 minute. Gene expression level was analyzed using the comparative threshold cycle method. GAPDH was used as the housekeeping gene.

Western blot

Cell was lysed by RIPA buffer with 1% PMSF (Sigma-Aldrich), 1% protease inhibitor (Roche Applied Science) and 1% phosphatase inhibitor (Cell Signaling Technology, MA, USA). Protein extracts were separated by sodium dodecyl sulfate-polyacrylamide gel electrophoresis (SDS-PAGE) and transferred to Immobilon-P PVDF Membrane (Merck Millipore, CA, USA) using Semi-Dry Electrophoretic Transfer Cell (Bio-Rad). After incubation with blocking buffer for one h, membrane was incubated with NOX5 antibodies (Santa Cruz Biotechnology, TX, USA), Phospho-Akt (Ser473) antibodies (Cell Signaling Technology), Phospho-Erk1/2 (Thr202/Tyr204) antibodies (Cell Signaling Technology), N-cadherin (CDH2) antibodies (Cell Signaling Technology), and β-actin antibodies (Santa Cruz Biotechnology) overnight at 4°C. Then, the membrane was incubated with secondary antibodies (ThermoFisher Scientific, MA, USA) for an hour at room temperature. Reactive proteins were visualized by WesternBright ECL Spray (advansta, CA, USA).

Dihydroethidium (DHE) staining

Superoxide content was determined by DHE (ThermoFisher Scientific) staining. Superoxide oxidized DHE to generate 2-hydroxyethidium (EOH) with red fluorescence. Cell was trypsinized and stained with 10 μM DHE in PBS for 15 min. Then, the fluorescence was detected by flow cytometry.

Lucigenin-induced chemiluminescence

Superoxide level was detected by lucigenin (Sigma-Aldrich), a chemiluminescent probe. Cells were incubated in HBSS buffer (Gibco) containing 50 μM lucigenin. Lucigenin-induced chemiluminescence was measured on Varioskan LUX Multimode Microplate Reader (ThermoFisher Scientific).

Cell proliferation assay

Cell proliferation was real-time monitored on xCELLigence Real-Time Cell Analyzer (ACEA Biosciences Inc., CA, USA). Cells were seeded on E-Plate 16 (ACEA), and cell index was continuously determined.

Tumor xenograft model

All animal experiments were performed according to the institutional guidelines and were approved by the Institutional Committee on the Use of Live Animals in Teaching and Research (protocol no. 3840-15) at the Animal Laboratory, Department of Surgery, University of Hong Kong (Hong Kong, SAR, China). To generate tumor xenograft, NOX5α-overexpressing CAL27 cells and the corresponding mock controls (2 × 106 cells in 100 μl) were injected subcutaneously into the flanks of athymic nu/nu mice (5 weeks old, weight range: 18-22 g). Ketamine (87.5 mg/kg) plus xylazine (12.5 mg/kg) was used as anaesthetic before tumor inoculation. Tumor size was determined by callipers and tumor volume was calculated using the following formula: Volume (mm^3) = ($L \times W^2$)/2, where L is the length (mm) and W is the width (mm). Mice were sacrificed with an excessive dosage of pentobarbital (100-150 mg/kg; Alfasan International BV, Woerden, The Netherlands) and tumor were harvested and weighted.

Immunohistochemistry (IHC)

Tumor xenografts derived from NOX5α-overexpressing CAL27 cells and mock cells were fixed in formalin, embedded in paraffin, and cut into 4 μm sections. The expression levels of Ki-67, VEGF, LYVE-1, and CD31 in xenografts

were measured by IHC. Sections were subjected to antigen retrieval and peroxidase blocking, followed by incubation with Ki-67 antibodies (ABCAM, Cambridge, UK), VEGF antibodies (ABCAM), LYVE-1 antibodies (ABCAM), and CD31 antibodies (ABCAM). Staining was visualised using EnVision+/HRP, Rabbit kit (DAKO, CA, USA).

Cell migration and invasion assay

Cell migration and invasion were measured by using CIM-Plate 16 (ACEA) in xCELLigence Real-Time Cell Analyzer (ACEA Biosciences Inc.). The lower chamber of CIM-Plate 16 was fulfilled with complete medium. For invasion assay, the upper chamber was coated with Matrigel (BD Biosciences, CA, USA) in 1:50 dilution for 4 hours at 37°C. Then, cells were seeded into the upper chamber, and the cell index was continuously measured.

Wound healing assay

Cells were seeded into 24-well plates. After 24 hours, cell grown to about 80% confluence were scratched with a 1 ml pipette tips, followed by two wash with medium to get rid of the detached cells. Wound closure was monitored and imaged under the bright field microscope.

Flow cytometry analysis and cell sorting

Cells were resuspended in phosphate-buffered saline (PBS) with 2% FBS. Then, cells were stained with phycoerythrin (PE)-conjugated CD271 antibodies (Miltenyi Biotec, Bergisch Gladbach, Germany) or isotype control (Miltenyi Biotec) for 10 minutes in the dark at 2-8°C. After washing twice with PBS, cells were resuspended into 300 μL of PBS and fluorescence was measured by using CytoFLEX S flow cytometer (Beckman Coulter, Inc., IN, USA). Cell sorting was performed on a FACSAria SORP (BD Biosciences).

Chromatin immunoprecipitation (ChIP) assay

ChIP assay were carried out using SimpleChIP® Plus Sonication Chromatin IP Kit (Cell signaling). Cells were cross-linked by 1% (v/v) formaldehyde (Sigma-Aldrich) for 10 minutes at 37°C. Then, DNA was sonicated and sheared to a length between 200 bp and 1000 bp. The sheared chromatin was incubated with NRF2 antibody (ABCAM) or rabbit IgG (Santa Cruz Biotechnology) overnight at 4°C. After purification, the DNA was subjected to QPCR to detect CD271 promoter fragment using QuantiNova SYBR Green PCR Kit (QIAGEN, CA, USA) on a LightCycler® 480 (Roche Applied Science). PCR conditions were as follows: 40 cycles of 95°C for 5 seconds and 60°C for 10 seconds. The primer sequence was as follows: Forward, 5'-TTGAACCAAGGAGACGGAGG-3'; Reverse, 5'-GGGGATTCATGCAGCTCCTT-3'. ChIP results were presented as a ratio of the concentration of immunoprecipitated DNA to input DNA (% input).

Sphere formation

The sorted $CD271^+$ and $CD271^-$ cells were suspended in DMEM/F12 medium (Gibco) supplemented with B27 (1:50, Gibco), 20 ng/ml EGF (ThermoFisher Scientific), 20 ng/ml basic FGF (ThermoFisher Scientific) and seeded in 96-well plate. After culturing for 7 days, the number of sphere was counted under a microscope.

Sulforhodamine B (SRB) in vitro toxicology assay

Cells were seeded in 96-well plate and treated by 2-8 μM cisplatin for 72 hours. The relative cell viability was determined using an in vitro Toxicology Assay Kit Sulforhodamine B (SRB) assay (TOX6; Sigma-Aldrich) according to the manufacturer's protocol. Wells with culture medium only were used as the negative control. The absorbance was measured using Varioskan LUX Multimode Microplate Reader (ThermoFisher Scientific). The percentage of viable cells was calculated as follows: $(OD_{\text{cisplatin-treated}} - OD_{\text{negative control}})/(OD_{\text{untreated control}} - OD_{\text{negative control}}) \times 100\%$.

AlamarBlue™ cell viability assay

Cells were seeded in 96-well plates and treated by 2 μM cisplatin for 72 hours. Cell viability was determined by alamarBlue™ Cell Viability Reagent (ThermoFisher Scientific). AlamarBlue (10 μl) was added to each well and the plate was incubated for 1 hour in cell culture incubator. Wells with culture medium only were used as the negative control. Relative fluorescence units (RFU) were determined by Amersham™ Typhoon5 Biomolecular Imager (GE Healthcare, IL, USA). The percentage of viable cells was cal-

culated as follows: ($RFU_{cisplatin\text{-}treated}$ - $RFU_{negative\ control}$)/($RFU_{untreated\ control}$ - $RFU_{negative\ control}$) × 100%.

Spheroid generation and cisplatin treatment

Cells were stained with Vybrant™ DiO Cell-Labeling Solution (ThermoFisher Scientific) and seeded in 384-well Black/Clear Round Bottom Ultra-Low Attachment Spheroid Microplate (Corning Inc., NY, USA). After 48 hours, spheroids were treated by 4 μM cisplatin for 8 days. Green fluorescence images of spheroids were acquired using IN Cell Analyzer 6500 HS (GE Healthcare, IL, USA). Images were acquired before the addition of cisplatin (0 day), 4 days and 8 days after the addition of cisplatin, respectively. The spheroid area was measured using ImageJ. Cisplatin cytotoxicity was presented as the changes in the spheroid area upon cisplatin treatment and was calculated using the following formula: The relative spheroid area = Spheroid $area_{cisplatin\text{-}treated}$/spheroid $area_{untreated\ control}$.

CD271 siRNA transfection

Cells were transfected with CD271 siRNA (10 nM, ThermoFisher Scientific) or negative control siRNA (10 nM) using HiPerFect Transfection Reagent (QIAGEN). The expression of CD271 was determined 72 hours after transfection.

Generation of NOX5-shRNA-expressing OTSCC cell lines

Two pairs of shRNA targeting different regions of NOX5 were designed. shRNA targeted conserved regions of all the reported NOX5 isoforms (alpha, beta, gamma, zeta, delta, epsilon). The sequences were as follows: shRNA-1-Forward, 5'-GATCCGCTACATCGATGGGCCTTATGCTTCCTGTCAGACATAAGGCCCATCGATGTAGCTTTTTG-3' shRNA-1-Reverse, 5'-AATTCAAAAAGCTACATCGATGGGCCTTATGTCTGACAGGAAGCATAAGGCCCATCGATGTAGCG-3' shRNA-2-Forward, 5'-GATCCGCGGTCTTTCGAGTGGTTTGTCTTCCTGTCAGAACAAACCACTCGAAAGACCGCTTTTTG-3' shRNA-2-Reverse, 5'-AATTCAAAAAGCGGTCTTTCGAGTGGTTTGTTCTGACAGGAAGACAAACCACTCGAAAGACCGCG-3' After annealing, the forward and reverse strands of shRNA template oligonucleotides were cloned into pGreenPuro™ Lentivector (System Biosciences). pPACKH1 HIV Lentivector Packaging Kit (System Biosciences) was used for lentivirus packaging. TransDux™ MAX Lentivirus Transduction Reagent (System Biosciences) was used for the lentivirus transduction of CAL27 and YD-38 cells.

NK cytotoxicity test

xCELLigence DP system (ACEA Biosciences Inc.) was used to measure NK cytotoxicity, as described by Moodley et al. [17]. Cells were seeded on E16 plates for 72 hours. Then, KHYG-1 cells were added to cancer cells at an effector to target (E:T) ratio of 3:1 or 6:1. The cell index of cancer cells was continuously measured. The percentage of cell lysis was calculated with the following formula: Cytotoxicity% = (cell $index_{no\ effector}$ - cell $index_{effector}$)/cell $index_{no\ effector}$) * 100%.

Spheroid model for NK cytotoxicity

Spheroid was generated for 48 hours, followed by the addition of KHYG-1 cells at an E:T ratio of 10:1. Green fluorescence images of spheroids were acquired using IN Cell Analyzer 6500 HS (GE Healthcare). Images were acquired before the addition of KHYG-1 (0 day), 4 days, 11 days and 12 days after the addition of KHYG-1, respectively. The spheroid area was measured using ImageJ. NK cytotoxicity was presented as the changes in the spheroid area upon NK treatment and was calculated using the following formula: The relative spheroid area = Spheroid $area_{NK\text{-}treated}$/spheroid $area_{untreated\ control}$.

Statistical analysis

Image data was analyzed by ImageJ. Microsoft Office Excel 2007 (IBM, New York, USA) was used for statistical analysis, and *p*-value less than 0.05 was regarded as statistically significant.

Results

NOX5α was the major NOX5 isoform in head and neck cancers

To identify the critical NOX members in head and neck cancer, we determined the expression of NOX family (NOX1-5 and DUOX1-2) in the head and neck cancer tissues in the patient cohort in The Cancer Genome Atlas (TCGA). Expression analysis from UALCAN (http://ualcan.path.uab.edu/index.html) showed that NOX2, NOX4, and NOX5 were up-regulated in

tumor tissues in comparison with normal (**Figure 1A**). NOX2 and NOX4 activation required a membrane-bound regulatory protein, p22-phox [12]. In contrast, NOX5 activity did not require additional subunits for the enzymatic activity [12]. Therefore, we speculated that NOX5 upregulation might alter the oxidative balance in head and neck cancers.

Mammalian cells expressed various NOX5 splice variants with various sizes. We evaluated the expression level of different NOX5 isoforms in the head and neck cancer tissues in TCGA. According to the records in ISOexpresso (http://wiki.tgilab.org/ISOexpresso/main.php), NOX5α was highly expressed in the head and neck cancer tissues (**Figure 1B**). Two different sizes of NOX5α exists in head and neck cancer tissues. The sequence for uc002arr.2 located at hg19 chr15:69,307,034-69,349,501 containing 16 exons. The uc010bif.2 was a NOX5α variant with sequence located at hg19 chr15: 69,323,942-69,349,501 containing 12 exons. NOX5α with 16 exons and 12 exons was expressed in 61.8% and 31.8% tumor tissue, respectively (**Figure 1B**). In contrast, NOX5γ was only detected in 6.4% tumor tissue. These results indicated that NOX5α is the major isoform expressed in head and neck cancer. Because of the remarkable increase of the NOX5α transcripts in the head and neck cancer tissues, we speculate that NOX5α plays an important part in OTSCC tumorigenesis.

NOX5α was a critical ROS-generating enzyme in OTSCC

As the superoxide-generating functions of NOX5α in oral cancer remain unclear, we first cloned the NOX5α sequences with 16 exons into the lentiviral vector and generated 2 different cell lines with stable NOX5α expression (**Figure 2A**, **2B**). DHE staining showed that the overall superoxide level was increased significantly in the NOX5α-overexpressing oral cancer cell lines (**Figure 2C**). Lucigenin-induced chemiluminescence confirmed these results (**Figure 2D**). The data suggested that NOX5α was a potent superoxide-generating enzyme in oral cancers.

NOX5α stimulated oral cancer proliferation and has a tumorigenic role in OTSCC

Given that superoxide could promote malignant transformation [18], we test whether superoxide-producing NOX5α increased the tumor-forming ability of OTSCC. NOX5α overexpression enhanced the proliferation rate of OTSCC cells (**Figure 3A**). NOX5α-overexpressing CAL27 cells and mock cells were injected subcutaneously into nude mice, and tumor growth was monitored. Xenograft volume over time and final tumor weight were significantly increased in NOX5α-overexpressing CAL27 cells in nude mice (**Figure 3B**). The results suggest a tumorigenic function of NOX5α in OTSCC. Immunohistochemical staining showed that xenograft developed from NOX5α-overexpressing CAL27 has a remarkable increase in proliferation marker (Ki-67) and angiogenic marker (VEGF) (**Figure 3C**). Since VEGF could promote the formation of blood vessels and increase lymphatic density [19], we further test the changes in blood vessel marker (CD31) and lymphatic endothelium marker (LYVE-1). An elevated expression level of CD31 and LYVE-1 was observed in xenograft from NOX5α-overexpressing CAL27 (**Figure 3C**), implicating that NOX5α could enhance vascular and lymphatic density.

ERK and AKT signaling pathways were known as oncogenic pathways regulated by superoxide [20, 21]. To investigate the mechanisms underlying the tumorigenic role of superoxide-producing NOX5α, we determine the phosphorylated level of ERK and AKT in NOX5α-overexpressing lines. An increase in phosphorylated ERK level was observed in NOX5α-overexpressing CAL27 and YD-38 cells (**Figure 3D**). In contrast, no obvious changes in AKT phosphorylation were observed in NOX5α-overexpressing OTSCC cells (**Figure 3D**).

NOX5α promoted migration and invasion in OTSCC

In light of the reported function of superoxide on tumor metastasis [18], we examined the functional influences of NOX5α on migration and invasion of oral cancers. We measured the migration and invasion property of the stable NOX5α-overexpressing OTSCC cell lines. Real-time migration and wound healing motility assay results indicated that the migratory ability of OTSCC cells increased significantly in NOX5α overexpression group (**Figure 4A**, **4B**). CAL27 cells have little invasive ability in the CIM-plate used in the real-time invasion assay. Compared with the control CAL27, the invasion ability increased remarkably in the NOX5α-

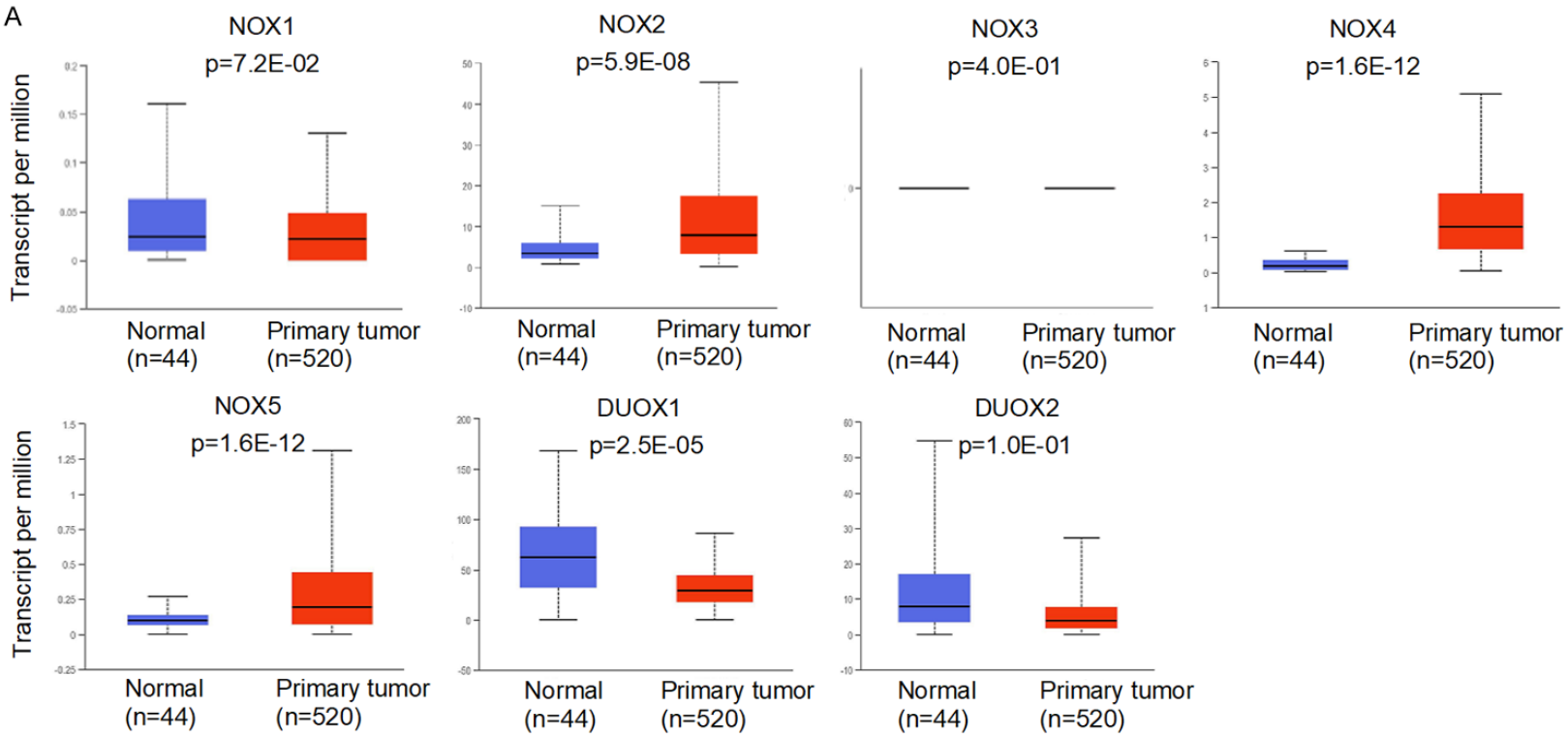

B

Isoforms		Median TPM and Percentage	Median TPM-based fold change
Alpha, 16 exons NM_001184779	Transcript variant 2 (uc002arr.2), mRNA	N: (0.039322; 100%) T: (0.093317; 61.8%)	1.4-fold up
Alpha, 12 exons NM_001184779	Transcript variant 2 (uc010bif.2), mRNA	N: T: (0.04809; 31.8%)	§
Gamma, 15 exons NM_024505	Transcript variant 1 (uc010bie.2), mRNA	N: T: (0.009673; 6.4%)	§

Figure 1. NOX5 expression was up-regulated in head and neck cancer tissues in TCGA dataset. A. Analysis of expression of NOX5 family in TCGA head and neck cancer dataset using UALCAN (http://ualcan.path.uab.edu/index.html). B. Analysis of isoform expression of NOX5 in TCGA head and neck cancer dataset using ISOexpresso (http://wiki.tgilab.org/ISOexpresso/main.php). TPM: Transcript per million. T: tumor, n=520. N: normal, n=44. Isoforms alpha (12 exons) and gamma (15 exons) are expressed in tumor samples but not in normal samples. Since the fold change cannot be expressed in numbers, it is denoted with "§".

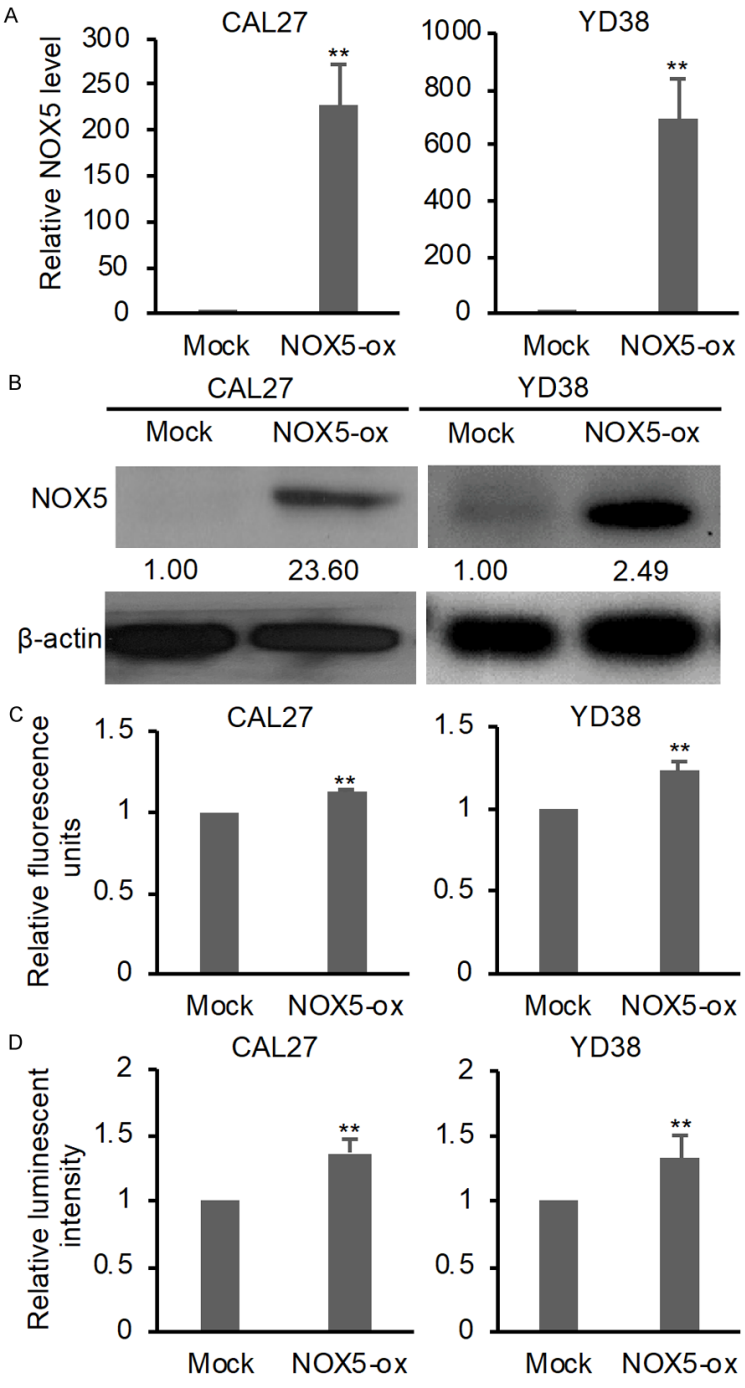

Figure 2. NOX5α expression increased the overall superoxide content in OTSCC. A. QPCR analysis of NOX5 expression in NOX5α-overexpressing (NOX5-ox) oral cancer cell lines (CAL27 and YD-38). B. Western blot analysis of NOX5 expression in NOX5α-overexpressing oral cancer cell lines (CAL27 and YD-38). Densitometry values of bands were determined using ImageJ software and were normalized to β-actin. Relative band intensities were displayed under each blot. C. Flow cytometry analysis of superoxide content in stable NOX5α-expressing oral cancer cell lines using DHE staining. D. Lucigenin-induced chemiluminescence analysis of superoxide content in stable NOX5α-expressing oral cancer cell lines. Data are expressed as mean ± SD (n=3). **P<0.01 (Student t test).

overexpressing cells (**Figure 4A**).

Epithelial-mesenchymal transition (EMT) conferred enhanced ability to migrate and invade in human cancer [22]. We investigated the regulatory role of NOX5α on the expression of EMT markers. N-cadherin (CDH2) expression was increased in mesenchymal cells. Alteration in CDH2 expression was associated with increased invasiveness [23]. CDH2 protein level was significantly increased in both CAL27 and YD-38 with stable NOX5α-overexpression (**Figure 4C**), implicating a mesenchymal phenotype of NOX5α-overexpressing cells.

Next, we addressed whether NOX5α increased migration and invasion via the generation of superoxide. NOX5α-overexpressing OTSCC cells were treated by tempol, a membrane-permeable free radical scavenging specific for superoxide. Tempol treatment significantly suppressed migratory and invasive ability in the NOX5α-overexpressing OTSCC (**Figure 4D**, **4E**), implicating that superoxide mediated enhanced migration and invasion.

NOX5α controlled the expression of CD271 in OTSCC

Results from QPCR showed that NOX5α overexpression increased CD271 transcription (**Figure 5A**). The percentage of $CD271^+$ cells was elevated in NOX5α-overexpressing OTSCC (**Figure 5B**). To explore whether superoxide generated by NOX5α mediated up-regulated CD271 expression, NOX5α-overexpressing

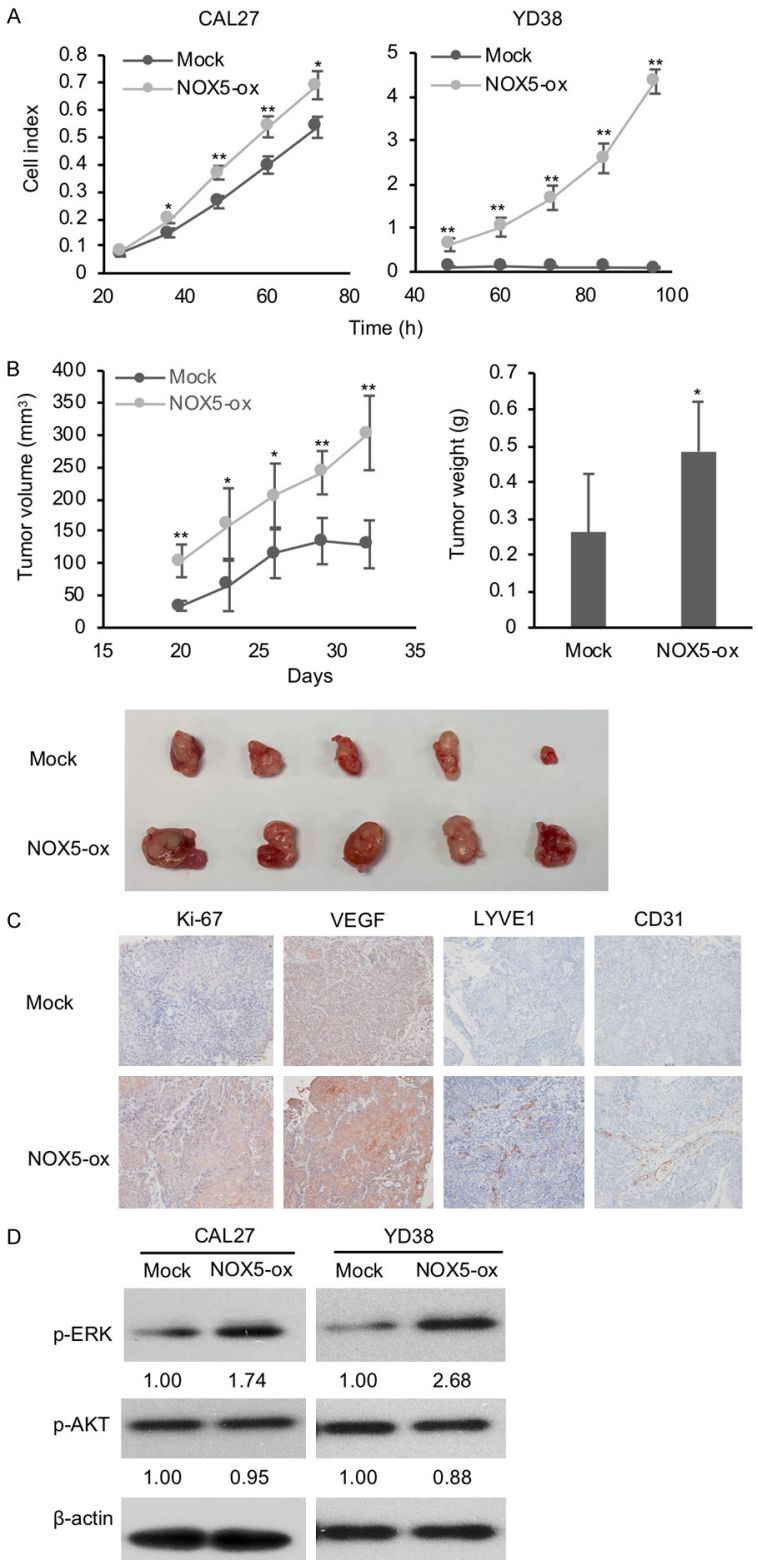

Figure 3. NOX5α increased tumorigenic properties of OTSCC and activated ERK signalling pathway. A. Real-time cell proliferation assay of NOX5α-overexpressing OTSCC cells. B. Tumor volume over time and final tumor weight of xenografts derived from NOX5α-overexpressing CAL27 cells. C. Immunohistochemical staining of Ki-67, VEGF, LYVE-1 and CD31 in xenografts derived from NOX5α-overexpressing CAL27 cells. D. Western blot analysis of ERK and AKT phosphoarylation in NOX5α-overexpressing OTSCC cells. Densitometry values of bands were determined using ImageJ software and were normalized to β-actin. Relative band intensities were displayed under each blot. Data are expressed as mean ± SD (n=3 for A; n=5 for B). *P<0.05, **P<0.01 (Student t test).

OTSCC cells were treated by a superoxide scavenger, tempol. A decrease in CD271 mRNA level and percentage of $CD271^+$ cells was observed upon tempol treatment (**Figure 5C**, **5D**), implicating that NOX5α enhanced CD271 expression via producing superoxide.

In view of the regulatory role of NOX5α on superoxide generation and CD271 transcription, we investigated whether ROS-activated transcription factor controlled CD271 expression. Nuclear factor E2-related factor 2 (NRF2) is a transcription factor activated by ROS [24]. NRF2 binds to the antioxidant response element (ARE, TGACTCA) of target genes and activates their expression [25]. We performed in silico analysis and found that CD271 promoter contained 1 ARE situated at -2770~-2765 bp from the transcriptional start site (+1) (**Figure 5E**). To address whether endogenous NRF2 interacted with the predicted ARE in CD271 promoter, ChIP assay was done. ChIP assay showed a significant increase in the level of NRF2 binding to the ARE of CD271 promoter in comparison with IgG control (**Figure 5F**).

To further explore the association between NOX5 and CD271, $CD271^+$ cells were

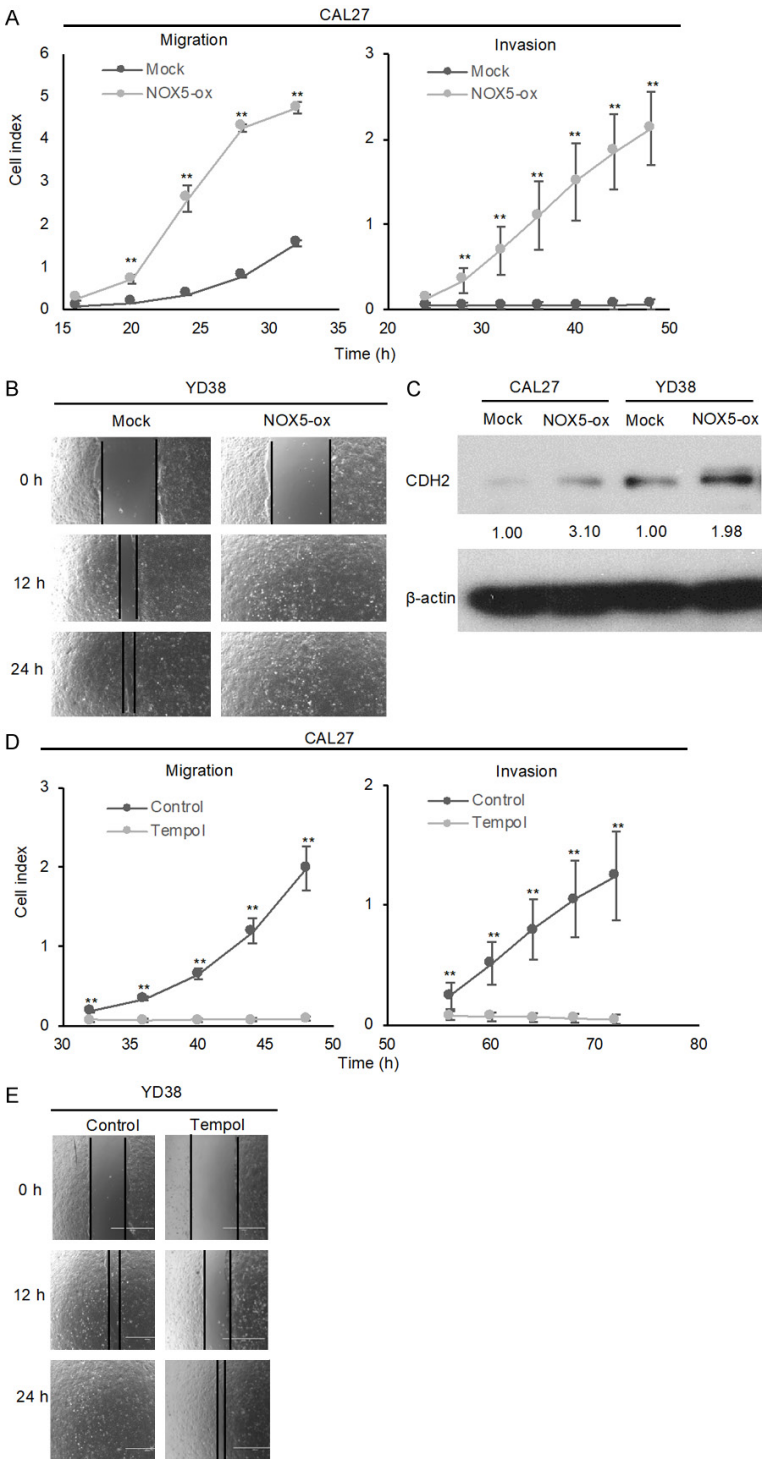

Figure 4. NOX5α promoted migration and invasion in OTSCC. A. Real-time monitor of migration and invasion of NOX5α-expressing CAL27 cells. B. Wound healing assays indicated that NOX5α-expressing YD-38 cells have a significantly higher migratory property. C. Western blot analysis of CDH2 in NOX5α-overexpressing OTSCC cells. Densitometry values of bands were determined using ImageJ software and were normalized to β-actin. Relative band intensities were displayed under each blot. D. Real-time monitor of migration and invasion of NOX5α-overexpressing CAL27 cells treated with tempol. E. Wound healing assays of migration of NOX5α-overexpressing YD-38 cells upon tempol treatment. Data are expressed as mean ± SD (n=3). **P<0.01 (Student t test).

sorted and the expression of NOX5 was measured. $CD271^+$ cells exhibited an increased expression of NOX5 compared to $CD271^-$ cells (**Figure 5G**). In addition, A higher expression level of OCT4, a stemness marker, was observed in $CD271^+$ cells (**Figure 5G**). The ability to form sphere was also enhanced in $CD271^+$ cells (**Figure 5H**).

NOX5α regulated the sensitivity of OTSCC cells to cisplatin

Given that $CD271^+$ cells were resistant to cisplatin treatment compared to $CD271^-$ cells [4], we evaluated whether NOX5α, the upstream regulator of CD271, regulated the sensitivity to cisplatin. The percentage of viable cells was higher in NOX5α-overexpressing OTSCC cells in comparison with mock cells (**Figure 6A**, **6B**) upon cisplatin treatment, indicating that NOX5α decreased the sensitivity to cisplatin.

Three-dimensional (3-D) spheroid model was further used to test cisplatin sensitivity. The spheroid model provided a method to mimic in vivo microenvironments such as structure of extracellular matrix surrounding tumor cells and the oxygen, nutrients, growth factors and proliferative gradients [26]. Compared to 2-D culture, spheroid culture shared the limited drug penetration properties with tumor mass [27]. Before cisplatin treatment, the spheroid areas of NOX5α-overexpressing cells were comparable to mock cells. After cisplatin treatment for 4 days, the spheroid area of mock cells began to decrease (**Figure 6C**). In contrast, there was no reduction in spheroid areas of NOX5α-

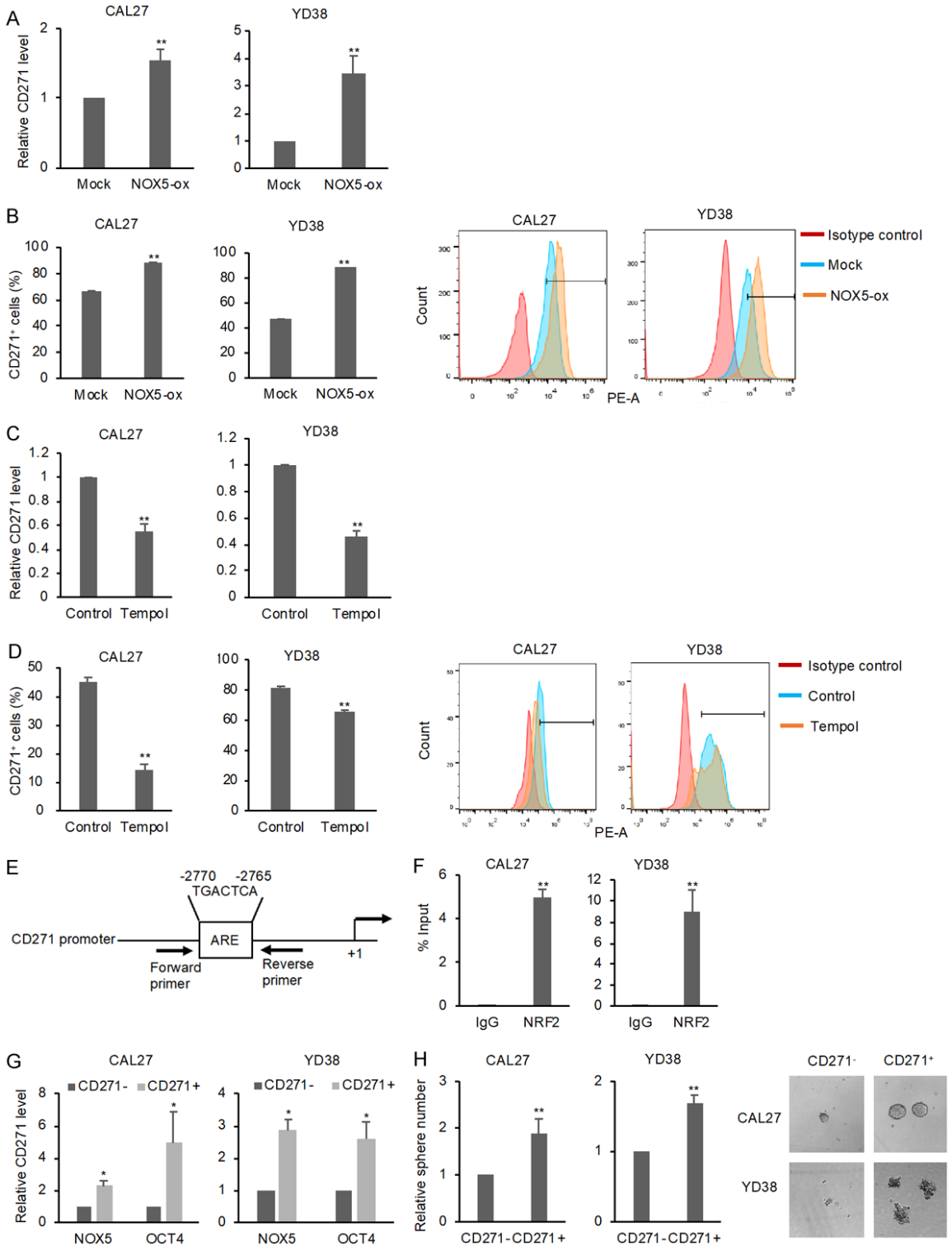

Figure 5. NOX5α was involved in CD271 up-regulation in OTSCC. A. QPCR analysis of CD271 expression in OTSCC cells with stable expression of NOX5α. B. Flow cytometry analysis of CD271 expression in OTSCC cells with stable expression of NOX5α. C. QPCR analysis of CD271 expression in OTSCC cells with stable expression of NOX5α treated by tempol. D. Flow cytometry analysis of CD271 expression in OTSCC cells with stable expression of NOX5α treated by tempol. E. Schematic representation of ARE in CD271 promoter. +1 indicated transcriptional start site. F. ChIP analysis of NRF2 binding to ARE in CD271 promoter. G. QPCR analysis of NOX5α and OCT4 expression in CD271+ and CD271- cells. H. Sphere formation assay of CD271+ and CD271- cells. Data are expressed as mean ± SD (n=3). *P<0.05, **P<0.01 (Student t test).

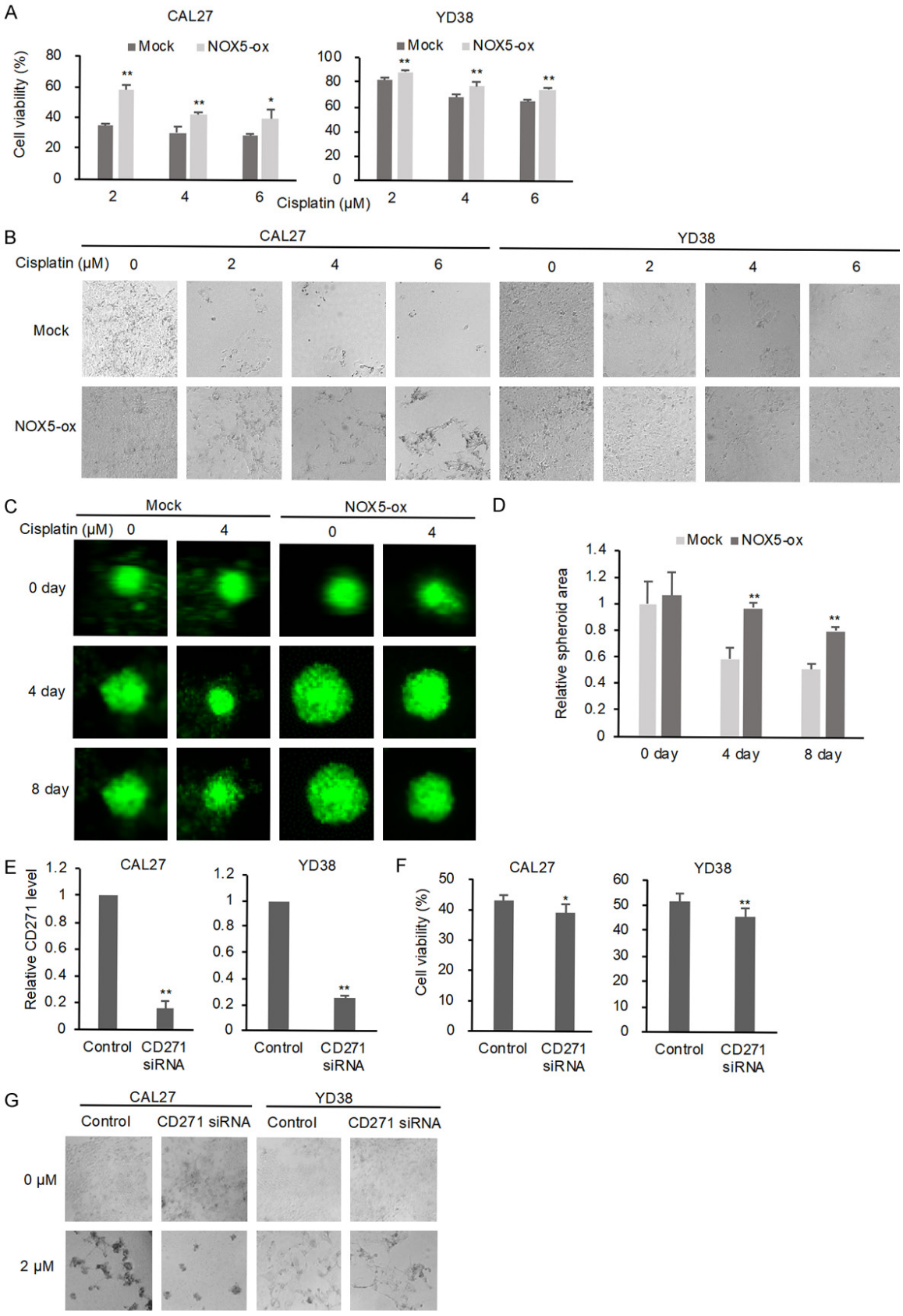

Figure 6. NOX5α reduced the sensitivity of OTSCC cells to cisplatin treatment. A. Viability of mock and NOX5α-overexpressing cells treated by cisplatin by using SRB assay. B. Representative images showing mock and NOX5α-

overexpressing cells treated by cisplatin. C. Fluorescent images of CAL27 spheroid upon cisplatin treatment. D. Relative spheroid area of CAL27 cells upon cisplatin treatment. E. QPCR analysis of CD271 expression in NOX5α-overexpressing cells transfected with CD271-siRNA. F. Viability of NOX5α-overexpressing cells transfected with CD271-siRNA in the presence or absence of cisplatin by using AlamarBlue™ Cell Viability assay. G. Representative images showing NOX5α-overexpressing cells transfected with CD271-siRNA in the presence or absence of cisplatin. Data are expressed as mean ± SD (n=3). *P<0.05, **P<0.01 (Student t test).

overexpressing cells. Eight days after cisplatin treatment, the spheroid area of NOX5α-overexpressing cells began to decrease (**Figure 6C**). A greater reduction in the spheroid area was observed in mock cells compared to NOX5α-overexpressing cells at both day 4 and day 8 (**Figure 6D**).

To explore whether NOX5α modulated cisplatin sensitivity via promoting CD271 expression, NOX5α-overexpressing OTSCC cells were transfected with CD271 siRNA and subjected to cisplatin treatment again. Knockdown of CD271 reduced the percentage of viable cells upon cisplatin treatment (**Figure 6E-G**), suggesting that CD271 mediated decreased cisplatin sensitivity.

NOX5α modulated the sensitivity of OTSCC cells to NK cell cytotoxicity

ROS could suppress the function of NK cells by inducing apoptosis [28]. Given the superoxide generation function of NOX5α, we addressed whether NOX5α affected the response to NK cell treatment. NOX5-shRNA-expressing OTSCC cells were generated (**Figure 7A**, **7B**) and subjected to KHYG-1 cell treatment. KHYG-1 cells caused greater inhibition of NOX5-knockdown cells compared to scrambled cells (**Figure 7C**, **7D**). In contrast, a reduced NK cell cytotoxicity was observed in NOX5α-overexpressing cells (**Figure 7E**, **7F**).

Compared to 2-D tumor cell culture, 3-D spheroid model possessed microenvironment and limited NK cell infiltrating properties reminiscent the situation found in solid tumors [29]. Therefore, NK cell cytotoxicity was further performed using 3-D spheroid model. Before the addition of KHYG-1 cells, NOX5α-overexpressing cells formed comparable spheroid in comparison with mock cells (**Figure 7G**). Four days after the addition of NK cells, a significant reduction in the spheroid area was observed in mock cells (**Figure 7G**). In contrast, the spheroid area of NOX5α-overexpressing cells was not altered by NK cells. After NK cell treatment for 11 days, the spheroid area of NOX5α-overexpressing cells began to decrease (**Figure 7G**). Mock cells exhibited a greater decrease in the spheroid area compared to NOX5α-overexpressing cells at all time points, including day 4, day 11, and day 12 (**Figure 7H**).

To address whether CD271 mediated reduced NK cell sensitivity, NOX5α-overexpressing cells transfected with CD271 siRNA were treated by KHYG-1 cells. An increased NK cytotoxicity was observed in CD271-knockdown cells in comparison with scramble cells (**Figure 7I**, **7J**).

Discussion

NOX5 is a member of the NADPH oxidase (NOX) family consisting of 7 highly conserved isoenzymes (NOX1, NOX2, NOX3, NOX4, NOX5, and DUOX1/2). Of which, NOX2, NOX4, and NOX5 were predominantly expressed in the TCGA head and neck cancers cohort. NOX5 has multiple splice variants. The expression of NOX5 variants in oral cancers and their tumorigenic role in OTSCC are unclear. The genomic location of NOX5 contains 18 exons encoding various splice variants [12]. The initial study from Bánfi B et al. suggested that these splice variants might have restricted tissue distribution [30]. We noted that the splice variant NOX5α (exons 3-18) is the most prevalent variant expressed in OTSCC. NOX5α is detected in normal spleen and lymph nodes [30]. High NOX5α expression is found in the peripheral blood cells of T-cell leukemia patients [31]. NOX5α is employed by human oncogenic retrovirus to maintain the transformed phenotype of T-cell lines [31]. In human T-cell leukemia virus type 1 (HTLV-1)-transformed cells, NOX5α activates the Jak-STAT5 cascade constitutively. In view of the potential oncogenic effects, we speculated that NOX5α might have regulatory functions on the key signaling pathways in OTSCC.

In OTSCC, we noted that NOX5α has strong tumor-promoting effects. This is likely to because of the activating effect on CD271 signaling in OTSCC. OTSCC with high NOX5α expres-

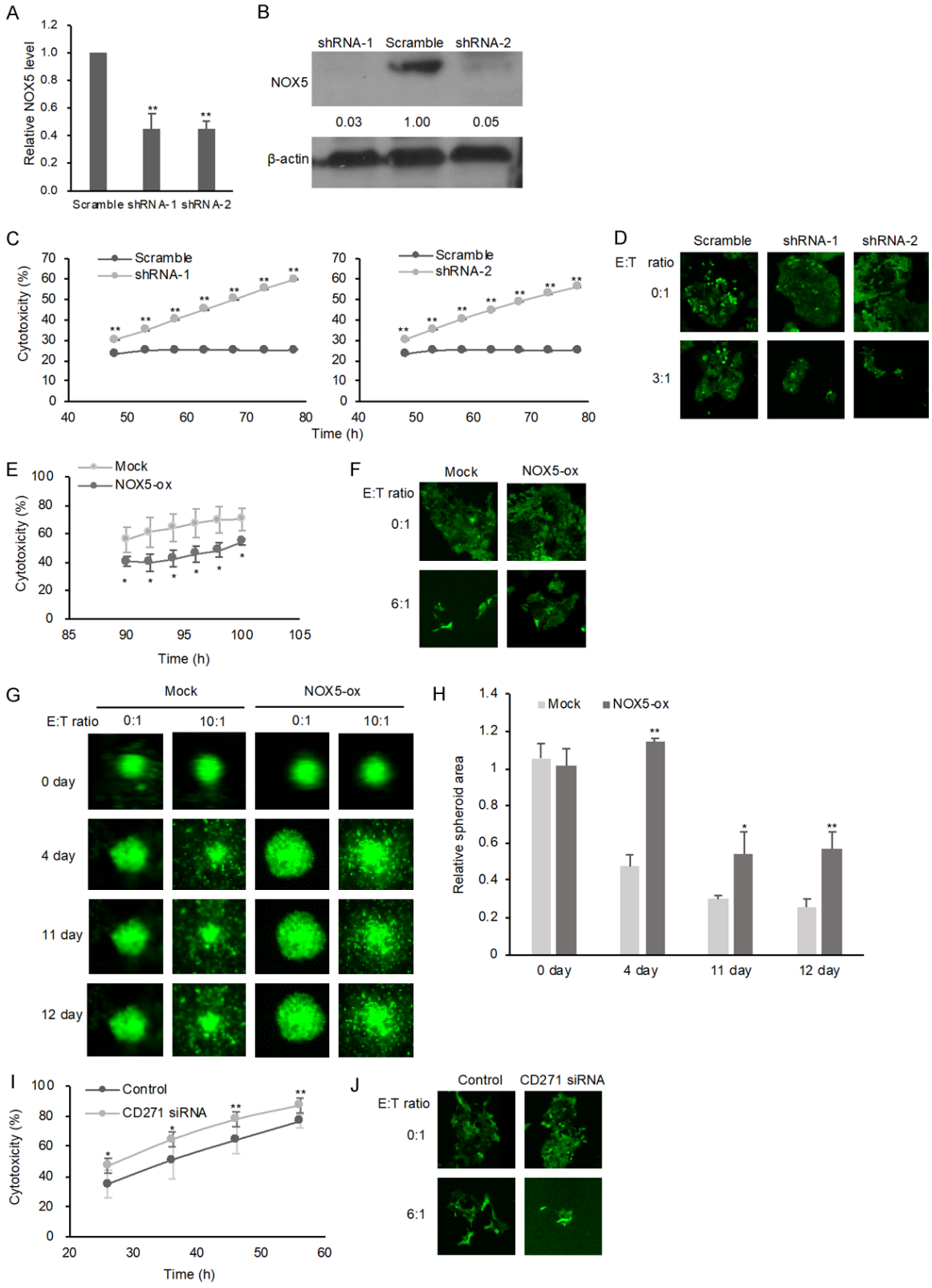

Figure 7. NOX5α decreased the sensitivity of OTSCC cells to NK cells. A. QPCR analysis of NOX5 expression in CAL27 cells expressing shRNA targeting NOX5. B. Western blot analysis of NOX5 expression in CAL27 cells expressing shRNA targeting NOX5. Densitometry values of bands were determined using ImageJ software and were normalized to β-actin. Relative band intensities were displayed under each blot. C. NK cell cytotoxicity toward CAL27 cells expressing shRNA targeting NOX5. CAL27 cells were co-cultured with KHYG-1 cells with a 3:1 E:T ratio. D. Represen-

tative images showing CAL27 cells expressing shRNA targeting NOX5 co-cultured with KHYG-1 cells with a 3:1 E:T ratio. E. NK cell cytotoxicity toward NOX5α-overexpressing CAL27 cells. CAL27 cells were co-cultured with KHYG-1 cells with a 6:1 E:T ratio. F. Representative images showing NOX5α-overexpressing CAL27 cells co-cultured with KHYG-1 cells with a 6:1 E:T ratio. G. Fluorescent images of CAL27 spheroid co-cultured with KHYG-1 cells at a 10:1 E:T ratio. H. Relative spheroid area of CAL27 cells co-cultured with KHYG-1 cells at a 10:1 E:T ratio. I. NK cell cytotoxicity toward NOX5α-overexpressing CAL27 cells in the presence of CD271-siRNA. CAL27 cells were co-cultured with KHYG-1 cells with a 6:1 E:T ratio. J. Representative images showing NOX5α-overexpressing CAL27 cells co-cultured with KHYG-1 cells with a 6:1 E:T ratio in the presence of CD271-siRNA. Data are expressed as mean ± SD (n=3). *P<0.05, **P<0.01 (Student t test).

sion form larger tumors in nude mice. Also, NOX5α increases proliferation, invasion, migration of oral caners. The tumor-promoting functions of NOX5α is mediated through the ROS-generating function in OTSCC. The previous study suggested that CD271-expressing HNSCC are resistant to cisplatin. CD271 was first recognized as a neurotrophin receptor. Later, it was found that CD271 is a marker for mammalian neural crest stem cells [32]. In oral cancer, CD271 overexpression promotes tumor invasion and nodal metastasis [33]. Our recent works reveal that CD271 singling increases stem cell marker expression and reduce chemotherapy sensitivity [34]. Several CD271 ligands (e.g., NGF, BDNF, NT3/4) have been discovered. Thus, the strong tumor-promoting effects of NOX5α observed in our OTSCC might possibly because of the enrichment of CD271-expressing OTSCC [2].

CD271 can be detected in the basal layer of normal human oral keratinocyte stem/progenitor cells and cancerous tissues [2, 35]. High CD271 expression is a marker of invasion and poor prognostic for oral cancer [3]. Comparing with clinical staging (TNM) and histopathological grading, CD271 had higher prognostic significance in oral cancer patients [36]. Recently, Morita et al. generated a monoclonal antibody for human CDD271 [37, 38]. They found that targeting CD271 in head and neck squamous cell carcinoma can enhance antibody-dependent cell-mediated cytotoxicity (ADCC) activity of natural killer (NK) cells [37]. Although there is clear evidence suggesting the clinical significance of CD271 in epithelial cancers in head and neck regions, the mechanisms governing CD271 up-regulation remains unclear.

Given that CD271 activates mitogen-activated protein kinase (MAPK)/extracellular signal-regulated kinase (ERK)1/2 pathway in head and neck squamous cell carcinoma, we speculated that NOX5α could also increase ERK phosphorylation in OTSCC [39]. MAPK/ERK pathways are frequently dysregulated in oral cancers upon stimulation from growth factors and hormones [40]. MARK/ERK signaling activates transcription factors involved in the proliferation, differentiation, angiogenesis, and metabolism of oral cancers [40, 41]. High p-ERK was associated with shorter disease-free survival in head and neck cancer patients treated with concurrent chemoradiation [42]. ERK signaling can protect oxidative stress-induced cell death by increasing antioxidant expression [43]. Further, ERK signaling affects the effectiveness of cisplatin-based chemotherapy in head and neck cancer treatment [43]. Inhibiting ERK is potentially useful for overcoming cisplatin resistance in head and neck cancer [40]. In KRAS-mutant lung cancer cells, activated MAPK signaling affects the NK cell surveillance program. Thus, we questioned whether NOX5α expression in oral cancer would affect the responsiveness to cisplatin and NK cells.

NK cell is a cytotoxic lymphoid cell in the human innate immune system with the capability to recognize and kill tumor cells. NK cells can kill the target cells by producing cytokines, releasing cytotoxic granules, and engaging to the death receptor on the cancer cells [44]. The pivotal role of NK cells in cancer progression has been demonstrated in various animal models. Animals will have a higher susceptibility to develop induced or spontaneous tumors when the functions of NK cells are disrupted [45]. It is now recognized that tumor development is resulting from the escape of cancer surveillance by NK cells. Evasion from the elimination of NK cells enables cancer to proliferate and spread at an early stage [46]. NK cells can locate and recognize the transformed cells as penetration of the infiltrating NK cells has been shown in a number of solid cancer models. An important strategy employed by the cancer cells to dampen NK cells cytotoxicity is by maintaining tumor microenvironment with high

inhibitory contents that suppress local NK cells activity [45, 46].

In vitro, squamous cell carcinoma is susceptible to NK cell-mediated lysis [47]. In clinical settings, however, the ability of NK cells to recognize and eliminate cancerous tissues is severely hampered. Infiltrating NK cells are distributed diffusely throughout the tumoral stroma of early oral cancers [48, 49]. Histological analysis shows that the tumor-infiltrating NK cells in oral lesions are functionally compromised with high expression of inactivation markers [50]. Although increasing data suggest that oral cancer might profoundly inhibit the cytotoxic functions of NK cells, the mechanism employed by head and neck cancer to inhibit NK cells remains to be elusive [50]. NOX5 activity affects extracellular ROS in the tumor microenvironment [51]. Nakamura et al. suggest that NK cell activity is inhibited by ROS [52]. Further. ROS can change the surface charge of NK cells and prevent their adhesion to the cancer cells [52]. Further, high ROS content in the tumor microenvironment could impair NK cells function. Our data suggest that NOX5α over-expressing OTSCC have a higher resistance to the cytotoxic action of NK cells. Targeting NOX5α activity may be useful to activate or improve the NK cell surveillance program in oral cancer patients.

Overall, our findings suggest that oral cancer expressed a unique NOX5 isoform. Increased NOX5α is associated with the increased expression of functional tumor-initiating cell marker CD271. CD271 expression is unregulated at transcription level mediated by NOX5α/ROS signaling. Increased oxidative stress modulated by NOX5α is a potent tumor promoter and contributor, which reduces the sensitivity of oral cancer cells to chemotherapy and NK cells. Further study is warranted to investigate the potential therapeutic value of targeting NOX5α in oral cancer treatment.

Acknowledgements

This work was supported by the Health and Medical Research Fund (HMRF) granted by Food and Health Bureau, Hong Kong Special Administrative Region (Project No. 03143326; 06173386), General Research Fund of Hong Kong SAR (Project No. 17115417), Seed Funding of Basic Research from The University of Hong Kong, Seed Fund for Translational and Applied Research from The University of Hong Kong.

Disclosure of conflict of interest

None.

Address correspondence to: Thian-Sze Wong, Department of Surgery, LKS Faculty of Medicine, The University of Hong Kong, Hong Kong, China. Tel: (852) 3917 9604; Fax: (852) 3917 9634; E-mail: thiansze@gmail.com

References

[1] Mackenzie IC. Growth of malignant oral epithelial stem cells after seeding intoorganotypical cultures of normal mucosa. J Oral Pathol Med 2004; 33: 71-78.

[2] Nakamura T, Endo K and Kinoshita S. Identification of human oral keratinocyte stem/progenitor cells by neurotrophin receptor p75 and the role of neurotrophin/p75 signaling. Stem Cells 2007; 25: 628-638.

[3] Kiyosue T, Kawano S, Matsubara R, Goto Y, Hirano M, Jinno T, Toyoshima T, Kitamura R, Oobu K and Nakamura S. Immunohistochemical location of the p75 neurotrophin receptor (p75NTR) in oral leukoplakia and oral squamous cell carcinoma. Int J Clin Oncol 2013; 18: 154-163.

[4] Imai T, Tamai K, Oizumi S, Oyama K, Yamaguchi K, Sato I, Satoh K, Matsuura K, Saijo S, Sugamura K and Tanaka N. CD271 defines a stem cell-like population in hypopharyngeal cancer. PLoS One 2013; 8: e62002.

[5] Korde SD, Basak A, Chaudhary M, Goyal M and Vagga A. Enhanced nitrosative and oxidative stress with decreased total antioxidant capacity in patients with oral precancer and oral squamous cell carcinoma. Oncology 2011; 80: 382-389.

[6] Maulik N. Redox signaling of angiogenesis. Antioxid Redox Signal 2002; 4: 805-815.

[7] Srivastava KC, Austin RD and Shrivastava D. Evaluation of oxidant-antioxidant status in tissue samples in oral cancer: a case control study. Dent Res J (Isfahan) 2016; 13: 181-187.

[8] Liu R, Wang HL, Deng MJ, Wen XJ, Mo YY, Chen FM, Zou CL, Duan WF, Li L and Nie X. Melatonin inhibits reactive oxygen species-driven proliferation, epithelial-mesenchymal transition, and vasculogenic mimicry in oral cancer. Oxid Med Cell Longev 2018; 2018: 3510970.

[9] Capote-Moreno A, Ramos E, Egea J, López-Muñoz F, Gil-Martín E and Romero A. Potential of melatonin as adjuvant therapy of oral cancer in the era of epigenomics. Cancers (Basel) 2019; 11.

[10] Brandes RP, Weissmann N and Schröder K. NOX family NADPH oxidases: molecular mechanisms of activation. Free Radic Biol Med 2014; 76: 208-226.
[11] Roy K, Wu Y, Meitzler JL, Juhasz A, Liu H, Jiang G, Lu J, Antony S and Doroshow JH. NADPH oxidases and cancer. Clin Sci (Lond) 2015; 128: 863-875.
[12] Bedard K, Jaquet V and Krause KH. NOX5: from basic biology to signaling and disease. Free Radic Biol Med 2012; 52: 725-734.
[13] Touyz RM, Anagnostopoulou A, Camargo LL, Rios FJ and Montezano AC. Vascular biology of superoxide-generating NADPH oxidase 5-implications in hypertension and cardiovascular disease. Antioxid Redox Signal 2019; 30: 1027-1040.
[14] Brar SS, Corbin Z, Kennedy TP, Hemendinger R, Thornton L, Bommarius B, Arnold RS, Whorton AR, Sturrock AB, Huecksteadt TP, Quinn MT, Krenitsky K, Ardie KG, Lambeth JD and Hoidal JR. NOX5 NAD(P)H oxidase regulates growth and apoptosis in DU 145 prostate cancer cells. Am J Physiol Cell Physiol 2003; 285: C353-369.
[15] Dho SH, Kim JY, Lee KP, Kwon ES, Lim JC, Kim CJ, Jeong D and Kwon KS. STAT5A-mediated NOX5-L expression promotes the proliferation and metastasis of breast cancer cells. Exp Cell Res 2017; 351: 51-58.
[16] Qian X, Nie X, Yao W, Klinghammer K, Sudhoff H, Kaufmann AM and Albers AE. Reactive oxygen species in cancer stem cells of head and neck squamous cancer. Semin Cancer Biol 2018; 53: 248-257.
[17] Moodley K, Angel CE, Glass M and Graham ES. Real-time profiling of NK cell killing of human astrocytes using xCELLigence technology. J Neurosci Methods 2011; 200: 173-180.
[18] López-Lázaro M. Excessive superoxide anion generation plays a key role in carcinogenesis. Int J Cance 2007; 120: 1378-1380.
[19] Koukourakis MI, Giatromanolaki A, Sivridis E, Simopoulos C, Gatter KC, Harris AL and Jackson DG. LYVE-1 immunohistochemical assessment of lymphangiogenesis in endometrial and lung cancer. J Clin Pathol 2005; 58: 202-206.
[20] Huang WC, Chio CC, Chi KH, Wu HM and Lin WW. Superoxide anion-dependent Raf/MEK/ERK activation by peroxisome proliferator activated receptor gamma agonists 15-deoxy-delta(12,14)-prostaglandin J(2), ciglitazone, and GW1929. Exp Cell Res 2002; 277: 192-200.
[21] Lim S and Clément MV. Phosphorylation of the survival kinase Akt by superoxide is dependent on an ascorbate-reversible oxidation of PTEN. Free Radic Biol Med 2007; 42: 1178-1192.
[22] Roche J. The epithelial-to-mesenchymal transition in cancer. Cancers (Basel) 2018; 10.
[23] Škovierová H, Okajčeková T, Strnádel J, Vidomanová E and Halašová E. Molecular regulation of epithelial-to-mesenchymal transition in tumorigenesis (Review). Int J Mol Med 2018; 41: 1187-1200.
[24] Tonelli C, Chio IIC and Tuveson DA. Transcriptional regulation by Nrf2. Antioxid Redox Signal 2018; 29: 1727-1745.
[25] Hirotsu Y, Katsuoka F, Funayama R, Nagashima T, Nishida Y, Nakayama K, Engel JD and Yamamoto M. Nrf2-MafG heterodimers contribute globally to antioxidant and metabolic networks. Nucleic Acids Res 2012; 40: 10228-10239.
[26] Edmondson R, Broglie JJ, Adcock AF and Yang L. Three-dimensional cell culture systems and their applications in drug discovery and cell-based biosensors. Assay Drug Dev Technol 2014; 12: 207-218.
[27] Perche F and Torchilin VP. Cancer cell spheroids as a model to evaluate chemotherapy protocols. Cancer Biol Ther 2012; 13: 1205-1213.
[28] Mellqvist UH, Hansson M, Brune M, Dahlgren C, Hermodsson S and Hellstrand K. Natural killer cell dysfunction and apoptosis induced by chronic myelogenous leukemia cells: role of reactive oxygen species and regulation by histamine. Blood 2000; 96: 1961-1968.
[29] Giannattasio A, Weil S, Kloess S, Ansari N, Stelzer EH, Cerwenka A, Steinle A, Koehl U and Koch J. Cytotoxicity and infiltration of human NK cells in in vivo-like tumor spheroids. BMC Cancer 2015; 15: 351.
[30] Bánfi B, Molnár G, Maturana A, Steger K, Hegedûs B, Demaurex N and Krause KH. A Ca(2+)-activated NADPH oxidase in testis, spleen, and lymph nodes. J Biol Chem 2001; 276: 37594-37601.
[31] Shigemura T, Shiohara M, Kato M, Furuta S, Kaneda K, Morishita K, Hasegawa H, Fujii M, Gorlach A, Koike K and Kamata T. Superoxide-generating Nox5α is functionally required for the human T-cell leukemia virus type 1-induced cell transformation phenotype. J Virol 2015; 89: 9080-9089.
[32] Morrison SJ, White PM, Zock C and Anderson DJ. Prospective identification, isolation by flow cytometry, and in vivo self-renewal of multipotent mammalian neural crest stem cells. Cell 1999; 96: 737-749.
[33] Chung MK, Jung YH, Lee JK, Cho SY, Murillo-Sauca O, Uppaluri R, Shin JH and Sunwoo JB. CD271 confers an invasive and metastatic phenotype of head and neck squamous cell carcinoma through the upregulation of slug. Clin Cancer Res 2018; 24: 674-683.
[34] Gao W, Li JZ, Chen SQ, Chu CY, Chan JY and Wong TS. BEX3 contributes to cisplatin chemo-

resistance in nasopharyngeal carcinoma. Cancer Med 2017; 6: 439-451.
[35] Thompson SJ, Schatteman GC, Gown AM and Bothwell M. A monoclonal antibody against nerve growth factor receptor. Immunohistochemical analysis of normal and neoplastic human tissue. Am J Clin Pathol 1989; 92: 415-423.
[36] Søland TM, Brusevold IJ, Koppang HS, Schenck K and Bryne M. Nerve growth factor receptor (p75 NTR) and pattern of invasion predict poor prognosis in oral squamous cell carcinoma. Histopathology 2008; 53: 62-72.
[37] Morita S, Mochizuki M, Wada K, Shibuya R, Nakamura M, Yamaguchi K, Yamazaki T, Imai T, Asada Y, Matsuura K, Sugamura K, Katori Y, Satoh K and Tamai K. Humanized anti-CD271 monoclonal antibody exerts an anti-tumor effect by depleting cancer stem cells. Cancer Lett 2019; 461: 144-152.
[38] Morita S, Mochizuki M, Shibuya-Takahashi R, Nakamura-Shima M, Yamazaki T, Imai T, Asada Y, Matsuura K, Kawamura S, Yamaguchi K, Yasuda J, Sugamura K, Katori Y, Satoh K and Tamai K. Establishment of a monoclonal antibody that recognizes cysteine-rich domain 1 of human CD271. Monoclon Antib Immunodiagn Immunother 2020; 39: 6-11.
[39] Murillo-Sauca O, Chung MK, Shin JH, Karamboulas C, Kwok S, Jung YH, Oakley R, Tysome JR, Farnebo LO, Kaplan MJ, Sirjani D, Divi V, Holsinger FC, Tomeh C, Nichols A, Le QT, Colevas AD, Kong CS, Uppaluri R, Lewis JS Jr, Ailles LE and Sunwoo JB. CD271 is a functional and targetable marker of tumor-initiating cells in head and neck squamous cell carcinoma. Oncotarget 2014; 5: 6854-6866.
[40] Peng Q, Deng Z, Pan H, Gu L, Liu O and Tang Z. Mitogen-activated protein kinase signaling pathway in oral cancer. Oncol Lett 2018; 15: 1379-1388.
[41] Gough NR. Focus issue: recruiting players for a game of ERK. Sci Signal 2011; 4: eg9.
[42] Kong LR, Chua KN, Sim WJ, Ng HC, Bi C, Ho J, Nga ME, Pang YH, Ong WR, Soo RA, Huynh H, Chng WJ, Thiery JP and Goh BC. MEK inhibition overcomes cisplatin resistance conferred by SOS/MAPK pathway activation in squamous cell carcinoma. Mol Cancer Ther 2015; 14: 1750-1760.
[43] Zhang R, Piao MJ, Oh MC, Park JE, Shilnikova K, Moon YJ, Kim DH, Jung U, Kim IG and Hyun JW. Protective effect of an isoflavone, tectorigenin, against oxidative stress-induced cell death via catalase activation. J Cancer Prev 2016; 21: 257-263.
[44] Sungur CM and Murphy WJ. Positive and negative regulation by NK cells in cancer. Crit Rev Oncog 2014; 19: 57-66.
[45] Vesely MD, Kershaw MH, Schreiber RD and Smyth MJ. Natural innate and adaptive immunity to cancer. Annu Rev Immunol 2011; 29: 235-271.
[46] Miller JS. The biology of natural killer cells in cancer, infection, and pregnancy. Exp Hematol 2001; 29: 1157-1168.
[47] Heo DS, Snyderman C, Gollin SM, Pan S, Walker E, Deka R, Barnes EL, Johnson JT, Herberman RB and Whiteside TL. Biology, cytogenetics, and sensitivity to immunological effector cells of new head and neck squamous cell carcinoma lines. Cancer Res 1989; 49: 5167-5175.
[48] Katou F, Ohtani H, Watanabe Y, Nakayama T, Yoshie O and Hashimoto K. Differing phenotypes between intraepithelial and stromal lymphocytes in early-stage tongue cancer. Cancer Res 2007; 67: 11195-11201.
[49] Zancope E, Costa NL, Junqueira-Kipnis AP, Valadares MC, Silva TA, Leles CR, Mendonça EF and Batista AC. Differential infiltration of CD8+ and NK cells in lip and oral cavity squamous cell carcinoma. J Oral Pathol Med 2010; 39: 162-167.
[50] Xie L, Pries R, Kesselring R, Wulff S and Wollenberg B. Head and neck cancer triggers the internalization of TLR3 in natural killer cells. Int J Mol Med 2007; 20: 493-499.
[51] Kawahara T and Lambeth JD. Phosphatidylinositol (4,5)-bisphosphate modulates Nox5 localization via an N-terminal polybasic region. Mol Biol Cell 2008; 19: 4020-4031.
[52] Nakamura K and Matsunaga K. Susceptibility of natural killer (NK) cells to reactive oxygen species (ROS) and their restoration by the mimics of superoxide dismutase (SOD). Cancer Biother Radiopharm 1998; 13: 275-90.